# Exchange Striction Effects in MnO and MnS†

B. MOROSIN
*Sandia Laboratories, Albuquerque, New Mexico 87115*
(Received 21 April 1969)

Lattice constants of MnO and MnS have been measured as a function of temperature from 7 to 300°K. Below the Néel temperature, the fcc lattices undergo a trigonal distortion as well as a volume contraction. By subtracting the usual thermal expansion from this volume contraction, the isotropic exchange striction has been studied. For MnO below the Néel temperature ($T_N \cong 118$°K), good agreement with the random-phase Green's-function theory previously developed to describe sublattice magnetization is obtained for the trigonal distortion; on the other hand, for the volume contraction, there are no theoretical results available for the region immediately below the Néel temperature to compare with the experimental next-nearest-neighbor spin-correlation curve which has been obtained. For MnS, below $T_N$ ($\cong 147$°K) the observed trigonal distortion was found to be a contraction along the [111] direction; the magnetization curves suggest, but do not positively prove, the absence of a biquadratic-exchange effect.

## I. INTRODUCTION

SLIGHT departures from the fcc symmetry of the NaCl lattice for iron-group oxides were first reported by Tombs and Rooksby.[1] Greenwald and Smart[2] first suggested that these crystallographic deformations are a consequence of the exchange interactions which result from antiferromagnetic ordering. Subsequently, there has been considerable interest in the magnetic properties of these type-II fcc antiferromagnetic compounds; in particular, neutron[3,4] and x-ray[5] diffraction studies and theoretical investigations[6–8] have clarified the understanding of the magnetic properties of MnO and MnS. However, below room temperature, accurate lattice constants were not previously available for MnS, and more precise values were desirable to test theoretical calculations on MnO. In particular, x-ray diffraction measurements of the exchange-striction-induced trigonal distortion can yield a direct determination of the sign of the product of the nearest-neighbor (nn) exchange interaction $J_1$ and its logarithmic derivative with respect to interspin distance $\partial \ln J_1/\partial r$ for these kinds of antiferromagnets.[9] In addition, Lines and Jones[8] have pointed out that measurements on the shape of the magnetization curve as a function of temperature should be particularly useful for MnS, since it is probably the most suitable material in which to study biquadratic-exchange effects.

In Sec. II, the mechanism by which the lattice distorts in these type-II fcc antiferromagnetic compounds is reviewed, and the procedure used to remove normal thermal expansion from the lattice constants versus temperature measurements is outlined. Section III reports the experimental x-ray diffraction results on MnO and MnS. For MnO, the lattice constants and the trigonal distortion as a function of temperature have been measured with greater precision than has previously been reported.[5] The distortion and volume contraction in MnS are found to be an order of magnitude smaller than those in MnO. Section IV summarizes the magnetization-versus-temperature curves which have been obtained from these distortions for both salts. These results are in complete agreement with the conclusions of Lines and Jones[7] that biquadratic exchange does not have to be invoked to explain the magnetic properties of MnO; in addition, these results confirm the conclusion made by these same authors on the magnitude of the derivative of the exchange constant with respect to nn separations in MnS.[8]

## II. MODEL

Many of the iron-group simple compounds which belong to the fcc symmetry class of the NaCl lattice magnetically order at temperatures denoted as the Néel temperature $T_N$. The spin arrangement for these antiferromagnetic compounds has been shown to be of type II,[4] and in the ordered state, the lattice usually undergoes an exchange-striction-induced trigonal distortion. In such type-II fcc antiferromagnets this exchange-striction process proceeds as follows. The magnetic ordering consists of ferromagnetically aligned sheets of spins lying in (111) planes, while the spin directions of these sheets are arranged antiferromagnetically from plane to plane. The environment of each magnetic spin consists of six parallel-aligned and six antiparallel-aligned nn spins. The six parallel nn spins are located on the same ferromagnetic sheet as the reference spin; the six antiferromagnetic nn spins are arranged centrosymmetrically in sets of three in planes above and below the reference spin. When the nn exchange interaction $J_1$ is antiferromagnetic (negative) and if the exchange interaction decreases with increasing separation between the magnetic spins, i.e., $\partial \ln J_1/$

† Work supported by the U. S. Atomic Energy Commission.
[1] H. P. Rooksby, Nature **152**, 304 (1943); Acta Cryst. **1**, 226 (1948); N. C. Tombs and H. P. Rooksby, Nature **165**, 422 (1950).
[2] S. Greenwald and J. S. Smart, Nature **166**, 523 (1950); Phys. Rev. **82**, 113 (1951).
[3] C. G. Shull, W. A. Straussen, and E. O. Wollan, Phys. Rev. **83**, 333 (1951).
[4] W. L. Roth, Phys. Rev. **110**, 1333 (1958); **111**, 772 (1958).
[5] D. S. Rodbell, L. M. Osika, and P. E. Lawrence, J. Appl. Phys. **36**, 666 (1965).
[6] M. E. Lines, Phys. Rev. **139**, A1304 (1965).
[7] M. E. Lines and E. D. Jones, Phys. Rev. **139**, A1313 (1965), and references therein.
[8] M. E. Lines and E. D. Jones, Phys. Rev. **141**, 525 (1966).
[9] E. D. Jones and B. Morosin, Phys. Rev. **159**, 451 (1967).

$\partial r<0$, the system (magnetic plus elastic) will lower its energy by contracting along a [111] direction as has been observed in MnO, MnS, and GdAs.[1,8] For positive $\partial \ln J_1/\partial r$, an expansion along the [111] direction is energetically more favorable as has been observed in FeO.[1] Either trigonal distortion results in a decrease in six and an increase in the remaining six nn spin separations from the reference spin. The resulting crystallographic symmetry of the unit cell would properly be described as rhombohedral with an angle $\alpha$ near 60°; however, in this paper, the pseudocubic cell (four times the volume of the primitive cell) which has been found more convenient to use in previous studies has been retained and its angle $\alpha$ taken as $\pi/2\pm\Delta$, where $\Delta$ will generally be less than 1°. In addition, below $T_N$, an additional contraction of the pseudocubic cell edges, $\delta a/a$, may occur other than that expected from a thermal-expansion change. This volume-striction results from the interaction $J_2$ of the reference spin with the six next-nearest-neighbors (nnn) spins. For $\partial \ln J_2/\partial r<0$, a pure contraction is energetically more favorable; a pure expansion may be observed should $\partial \ln J_2/\partial r$ be positive.

Thus, assuming a small trigonal distortion, the resulting *equilibrium* angle $\Delta$ and *equilibrium* isotropic contraction $\delta a/a$ below $T_N$ are given by[6,10]

$$\Delta=-Nz_1J_1\epsilon_1(\langle \mathbf{S}_i\cdot\mathbf{S}_j\rangle_{\mathrm{nn}}{}^{p}-\langle \mathbf{S}_i\cdot\mathbf{S}_j\rangle_{\mathrm{nn}}{}^{a})/24C_{44} \quad (1)$$

and

$$\delta a/a=Nz_2J_2\epsilon_2\langle \mathbf{S}_i\cdot\mathbf{S}_j\rangle_{\mathrm{nnn}}/6(C_{11}+2C_{12}), \quad (2)$$

with

$$\epsilon_1=-r(\partial \ln J_1)/\partial r$$

and

$$\epsilon_2=-r(\partial \ln J_2)/\partial r, \quad (3)$$

where $z_1(=12)$ and $z_2(=6)$ are the number of nn and nnn spins, $N$ is the number of spins in the system, $\langle\cdots\rangle_{\mathrm{nn}}{}^{p}$, $\langle\cdots\rangle_{\mathrm{nn}}{}^{a}$, and $\langle\cdots\rangle_{\mathrm{nnn}}$ refer to thermal averages over parallel nn, antiparallel nn, and nnn, respectively, and $C_{11}$, $C_{12}$, and $C_{44}$ are the appropriate elastic constants.

Lines[6] has shown the molecular field estimate for nn interactions, $\langle \mathbf{S}_i\cdot\mathbf{S}_j\rangle_{\mathrm{nn}}{}^{p}=-\langle \mathbf{S}_i\cdot\mathbf{S}_j\rangle_{\mathrm{nn}}{}^{a}\cong(\bar{S})^2$, to be an acceptable approximation while, for nnn interactions $\langle \mathbf{S}_i\cdot\mathbf{S}_j\rangle_{\mathrm{nnn}}\cong(\bar{S})^2$ would be a poor approximation. He has shown that at $T_N$, $\langle \mathbf{S}_i\cdot\mathbf{S}_j\rangle_{\mathrm{nnn}}\approx 0.3S(S+1)$ for MnO and that this spin-correlation function has a $T^{-1}$ dependence in the paramagnetic region. The exact form for $\langle \mathbf{S}_i\cdot\mathbf{S}_j\rangle_{\mathrm{nnn}}$ below $T_N$ has yet to be calculated. Hence, Eq. (1) for the equilibrium angle may be expressed as

$$\Delta=-Nz_1J_1\epsilon_1(\bar{S})^2/12C_{44}, \quad (4)$$

while Eq. (2) for the isotropic contraction must be retained in its original form. It should be pointed out that $J_1$ and $J_2$ (and hence $\epsilon_1$ and $\epsilon_2$) are assumed to be temperature-independent.

[10] D. S. Rodbell and J. Owen, J. Appl. Phys. **35**, 1002 (1964).

From the measurement of the positions of diffraction peaks $2\theta$ at any temperature, the interatomic spacings between particular planes in the crystal may be determined, and these, in turn, may be related to the size $a$ and shape $\frac{1}{2}\pi+\Delta$ of the unit cell. In order to obtain the magnitude of any volume change due to magnetic interactions, the normal thermal expansion of the lattice must be subtracted. The procedure used is based on the Mie-Grüneisen equation of state and, hence, may require justification at very low temperatures. Grüneisen[11] derived the following relationship for thermal expansion of solids:

$$\frac{V-V_0}{V_0}=\frac{(E/Q)}{1-b(E/Q)}, \quad (5)$$

where $V$ and $V_0$ are the atomic volumes at any temperature and absolute zero, $E$ is the specific internal energy, and $b$ and $Q$ are parameters characteristic of the solid. We have the relation $b=(m+n+3)/6$, where $m$ and $n$ are the exponents in the attractive and repulsive terms in the Mie equation[11] relating the potential energy to the distance between vibrating atoms. The parameter $Q$ can be defined either in terms of specific heat $C_V$ and the volume coefficient of thermal expansion $\alpha$ or in terms of the Grüneisen parameter $\gamma$, bulk modulus $B$, and atomic volume in the following manner:

$$Q=C_V/\alpha=VB/\gamma. \quad (6)$$

Since $\Delta$ is very small, the crystal system is assumed to remain isotropic ($\delta a/a\cong\delta V/3V$ is good to 1 part in $10^4$) and, hence, in the above expression $\gamma$ does not have to be a tensor. On the other hand, it appears appropriate to comment on the temperature dependence of $\gamma$ since it is well known that $\gamma$ for some NaCl-structure-type solids changes significantly in the temperature range $0.1\Theta$–$0.2\Theta$, $\Theta$ being the Debye characteristic temperature. However, knowing the ratio of elastic stiffness $C_{44}/C_{11}$, and the elastic anisotropy $(C_{11}-C_{12})/2C_{44}$, an estimate of the behavior of $\gamma$ as a function of temperature can be made.

Rewriting Eq. (5), for a nonmagnetic solid

$$V(T)=V_0\left(1+\frac{(E/Q)}{1-b(E/Q)}\right), \quad (7)$$

it is possible to calculate the value of volume as a function of temperature provided values of $b$ and $Q$ are known. The value of $C_V$ and $E$ may be obtained using the Debye approximation.

Since $\delta a/a\cong\delta V/3V$, in the case involving a magnetic system, Eq. (7) may be written

$$V(T)_{\mathrm{mag}}=V_0\left(1+\frac{(E/Q)}{1-b(E/Q)}\right)-\tfrac{1}{3}f_{\delta V}, \quad (8)$$

[11] E. Grüneisen, Ann. Physik **39**, 257 (1912); G. Mie, Ann. Physik **11**, 657 (1903).

where $V_0$ is understood to be the volume at absolute zero *if the system were nonmagnetic* and $f_{\delta V}$ is a function of $\langle \mathbf{S}_i \cdot \mathbf{S}_j \rangle_{\text{nnn}}/S^2$, with $\langle \mathbf{S}_i \cdot \mathbf{S}_j \rangle_{\text{nnn}}$ inferred from Eq. (2) and $S$ equal to the saturation spin values at 0°K.

Thus experimental measurements can be used with Eq. (8) to determine $\delta a/a$ as a function of temperature independent of normal thermal expansion. The temperature dependence of $\delta a/a$ should yield the nnn's spin correlation curve below $T_N$. The temperature dependence of $\Delta$ yields the sublattice magnetization through $\bar{S}$ since $\bar{S}^2 = \langle \mathbf{S}_i \cdot \mathbf{S}_j \rangle_{\text{nn}}$, Eq. (4), and, thus, should be useful in determining the presence in these magnetic systems of an intrinsic biquadratic exchange, i.e., an interaction of the form $j_n(\mathbf{S}_i \cdot \mathbf{S}_j)^2$ in addition to the usual Heisenberg bilinear exchange of the form $J_n \mathbf{S}_i \cdot \mathbf{S}_j$, where $j_n$ and $J_n$ are, respectively, the biquadratic and bilinear exchange constants. Such a biquadratic effect would be manifested in a change in the falloff of the magnetization curves. However, to date, no experiments on MnO or MnS have required introduction of a biquadratic-exchange term for its theoretical interpretation.[2]

## III. EXPERIMENTAL

Room-temperature x-ray powder measurements on MnO and MnS were made using Cu $K\alpha$ ($\lambda_{K\alpha_1} = 1.54050$ Å) radiation and a 114.5-mm Norelco powder camera. For the low-temperature lattice constants, both powder and single crystal (kindly furnished by R. Lindsay) samples of MnO and powder MnS were examined with an x-ray diffraction cryostat described elsewhere.[12] In order to obtain better temperature control above 90°K, slurries of liquid nitrogen-Freon were used for the refrigerant and temperature measurements were performed with a copper-constantan thermocouple.

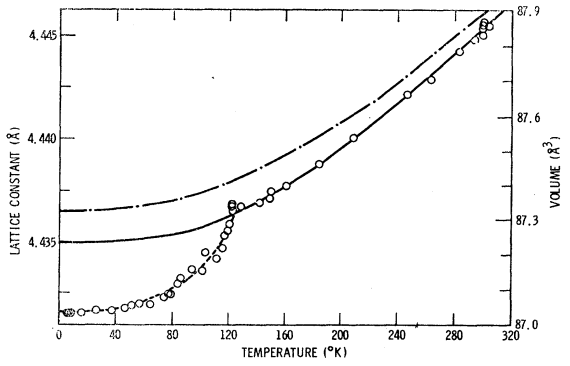


FIG. 1. Lattice constants (or volume; see text) for MnO between 7 and 300°K. The solid and broken curves are, respectively, the predicted values for a Debye solid ignoring nnn spin correlation in the paramagnetic region or including a contribution calculated by Lines (Ref. 6). Note that the "correct" Debye-solid curve is the broken one and that the data points for the magnetic solid must lie below it. The dashed line through experimental data points below $T_N$ is obtained from the trigonal distortion data (see text). Errors in measurements are approximately the size of the open circles.

[12] B. Morosin, J. Chem. Phys. 44, 252 (1966).

The most accurate measurements of the trigonal distortion are obtained by observing the splitting of the high $2\Theta$ lines even though those particular lines may not yield the direction of distortion from cubic symmetry. For example, with Cu $K\alpha$ radiation in the region of 160° $2\Theta$ for MnO, the diffraction peaks (doublet due to the small difference in wavelength for $\alpha_1$ and $\alpha_2$) corresponding to the (440) reflection each split into two peaks of equal magnitude and provide the most accurate measurement of the magnitude of distortion from cubic symmetry; however, the direction of distortion, that is, whether a contraction or elongation along the threefold axis occurs, is determined by diffraction peaks which split into peaks of unequal magnitude at lower values of $2\Theta$ such as those corresponding to the (333), (511), or (422) reflections.

For MnS, both copper and chromium radiation ($\lambda_{K\alpha_1} = 2.28962$ Å) were used in order to provide intense lines at high Bragg angle to obtain the direction and magnitude of the distortion. In this case the distortion is quite small and the diffraction peaks never become fully resolved. These overlapping peaks appear as broad-structured envelopes; these were machine fitted using the shape of resolved peaks which were observed above $T_N$. Although the distortion from cubic symmetry is small for MnS, it can be measured as a function of temperature and allows the direct observation that the unit cell is contracted along the threefold axis.

Room-temperature (23±1°C) lattice constants for MnO and MnS were determined to be 4.4457±0.0002 and 5.2233±0.0002 Å, respectively. These values for the lattice constants are in good agreement with previously published values.[13] At helium temperature the lattices become rhombohedral with the values 4.4316±0.0003 Å and 90.624±0.008°C for MnO and 5.1982±0.0004 Å and 90.099±0.015°C for MnS. For MnO these values may be compared with 4.437 Å and 90.43°C obtained by neutron diffraction[4] and 4.415 Å and 90.624°C obtained by previous x-ray diffraction[5] studies. Experimental results for the lattice constant as a function of temperature for MnO are given in Fig. 1; the curves shown on this figure will be explained later. The volume is equal to $a^3(1-3\cos^2\alpha+2\cos^3\alpha)^{-1/2}$. Figure 2 displays the temperature dependence of the distortion angle; these values are in good agreement with previous results.[5]

The corresponding experimental results for MnS are given in Figs. 3 and 4. Part of the scatter in our data points appears to be either a slight hysteresis in the mechanical change in the unit cell size of our powdered samples (compared to the single crystal MnO) or in the temperature-control system. On the other hand, the scatter of the data points about the smooth line in Fig. 4

[13] A. Iandelli, in *Rare Earth Research*, edited by V. Kleber (The Macmillan Co., New York, 1961).

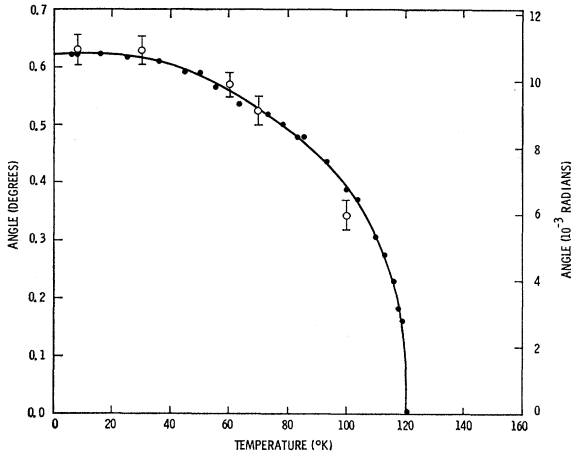


FIG. 2. The angle $\Delta$ of the pseudocubic unit cell, $\frac{1}{2}\pi+\Delta$, for MnO below $T_N$. The open circles are data of Rodbell, Osika, and Lawrence (Ref. 5). Errors in measurement are approximately $1\frac{1}{2}$ times the size of the solid points.

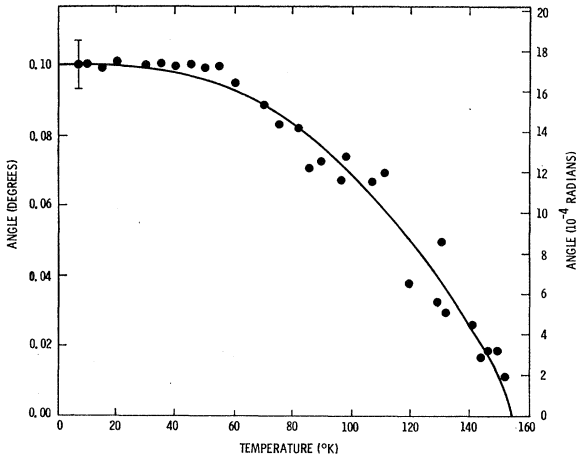


FIG. 4. The angle $\Delta$ of the pseudocubic unit cell, $\frac{1}{2}\pi+\Delta$, for MnS below $T_N$. The trigonal distortion in MnS is almost an order of magnitude smaller than that observed in MnO. Errors in measurements are indicated on the lowest-temperature point.

compared with Fig. 2 is a direct result of the much smaller distortion in MnS compared with that in MnO. Even so, the distortion in MnS is almost three times larger than that determined in GdAs.[9]

## IV. EXCHANGE STRICTION

Lines and Jones[7] have shown that the temperature dependence of the MnO magnetization curve, which previously had been considered anomalous, was not evidence for the existence of intrinsic biquadratic exchange in the MnO system. They used Green's-function and spin-wave techniques to examine and study in detail the effects which the exchange-induced distortion of the cubic lattice has on the magnetic properties of MnO, and they obtained quantitative agreement using a bilinear-exchange Hamiltonian in which the nn interaction constant takes the form $J_1 \pm j(\tilde{S})^2$ without invoking biquadratic terms. However, they were not able to show that biquadratic interactions are necessarily entirely absent because the shape of the magnetization curve for MnO proved to be rather insensitive to the presence of a small biquadratic term in addition to the observed trigonal distortion. On the other hand, they concluded that MnS should provide the system most suitable for detailed study to search for effects which might be due to biquadratic exchange.[8]

On Fig. 5, the values of $R_\Delta$, the square root of the ratio $\Delta(T)/\Delta(0°\text{K})$, where $\Delta(0°\text{K})$ is easily obtained from Fig. 2 by extrapolation, are shown on curves calculated by Lines and Jones (Fig. 7, Ref. 7) in the random-phase Green's-function approximation for MnO. In these curves $J_1$ is assumed to be equal to $J_2$.

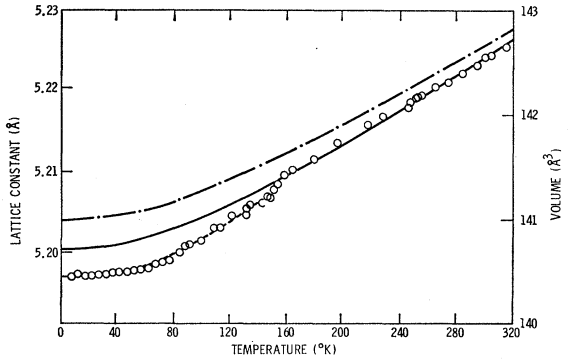


FIG. 3. Lattice constants (or volume; see text) for MnS between 7 and 310°K. The solid and broken curves are obtained in the same manner as those for Figure 1. Errors in measurements are approximately the size of the open circles.

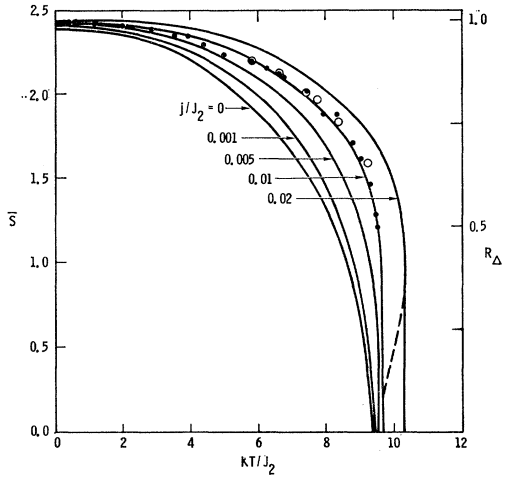


FIG. 5. Average spin per site $\bar{S}$ as a function of temperature $(kT/J_2)$, calculated by Lines and Jones (Ref. 7, Fig. 7) in the random-phase Green's-function approximation for MnO. The solid lines are calculated for various values of the distortion parameter $j/J_2$. The open circles are the neutron scattering intensities from [111] planes by G. G. Shull, W. A. Strausser, and E. O. Wollan, Phys. Rev. 83, 333 (1951); solid points are $R_\Delta$, where $R_\Delta=[\Delta(T)/\Delta(0°\text{K})]^{1/2}$ and $\Delta(T)$ are from Fig. 2 of this study.

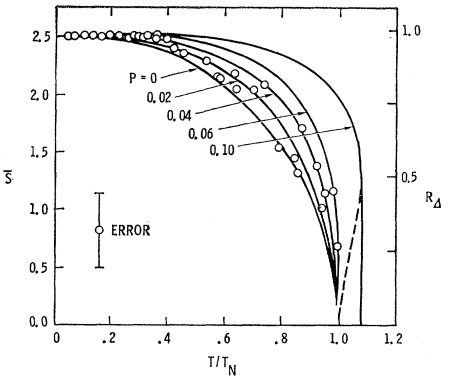


FIG. 6. Average spin per site $\bar{S}$ versus $T/T_N$ for MnS. Data, $R_\Delta=[\Delta(T)/\Delta(0°\text{K})]^{1/2}$ and $\Delta(T)$ from Fig. 4, are plotted on the curves calculated by Lines and Jones (Ref. 8, Fig. 1) in the molecular field approximation for spin $\frac{5}{2}$ and for various values of the "biquadratic parameter" $P$. Data points appear to scatter about the $P=0.02$ curve; however, experimental error is sufficiently large to negate such a conclusion.

With a slight adjustment of our temperature scale, the trigonal-distortion data fit closely the distortion parameter curve for $j/J_2=0.01$, in good agreement with the Lines and Jones fit of the few data available from neutron scattering intensities. This value may be compared with the value $j/J_2=0.009$ which is the contribution to be expected from the lattice distortion.[7] Because the present experimental data ranges over the entire temperature region up to $T_N$ compared to the few data points available to Lines and Jones, one may state without reservation that an excellent fit between theory and experiment has been obtained for MnO.

Even though experimental information available for MnS below $T_N$ was rather scant, Lines and Jones[8] singled out this salt as the one most suitable for detailed study of biquadratic-exchange effects. From the temperature dependence of $Mn^{55}$ NMR experiments, which provided information on the temperature dependence of sublattice magnetization, they concluded that a lattice distortion in MnS should be rather small. They further demonstrated that although the nn biquadratic exchange $j_1$ would be important, the nnn term, $j_2$, is fairly insensitive, allowing them to describe the NMR results in terms of $J_1$, $J_2$, $j_1$, and $\Delta$. By assuming $j_2=0$ and only nn and nnn interactions, the "biquadratic" parameter $P$ reduces to $P=j_1/J_2$ (the reader is referred to their paper for the complete expression of $P$). Hence in the absence of a large trigonal distortion, the behavior of biquadratic-exchange effects upon sublattice magnetization curves appears to yield similar results to those which are obtained by the statistical treatments (such as Green's function) of these salts including a distortion term $j/J_2$. Our experimental results on the temperature dependence of $R_\Delta$ for MnS are shown in Fig. 6. These results are plotted against the curves of Lines and Jones calculated for various values of the biquadratic parameter, $P$. In this case the experimental error is large enough to prevent stating, without reservation, that biquadratic-exchange effects are present in MnS. However, the data points appear to follow the $P=0.02$ curve much more closely than that for $P=0.0$. For MnS, the trigonal distortion $\Delta$ at 0°K is one order of magnitude smaller than found for MnO. The experimental data points do, in fact, follow the $j/J_2=0.001$ curve of Fig. 5 suggesting that in this salt, just as in MnO, the shape of the magnetization curve is dependent upon the distortion the lattice undergoes. These results agree with Lines and Jones's conclusion that the importance of biquadratic exchange in magnetically ordered systems could be considerably less than had previously been supposed.[8]

Let us now consider the volume contraction which has been observed in these salts. In order to obtain the magnetic volume striction from measurements on the unit cell edge, the usual thermal expansion of the solid must be taken into account. The procedure employed consists of fitting the experimental data by least-squares procedures to Eq. (8), rewritten in the form

$$V(T)_{\text{mag}}=V_0[1+AE/(1-BE)]-Df_{\delta V}, \qquad (9)$$

where $A$, $B$, $D$, and $V_0$ were considered unknowns, $f_{\delta V}$ a function of temperature, will be discussed below, and $E$, in the Debye approximation, is a function of $\Theta/T$. Note that at 0°K, the observed volume of the cell is equal to $V_0$ minus $D$, that $A$ and $B$ can be estimated from Eq. (6) and the term $b$ provided we can estimate the temperature dependence of $\gamma$, and that $\Theta$ can be estimated from the Lindemann relation,

$$T_m(\text{at.wt}\ a^2\Theta^2)^{-1}\approx 13\times 10^{10},$$

where $T_m$, at.wt, $a$, and $\Theta$ are the melting point atomic weight, unit cell edge, and Debye temperature, respectively. The latter relationship predicts $\Theta$ for MnO and MnS to be 425 and 275°K, respectively.[14]

Before the fit to Eq. (9) can be given, the form of $f_{\delta V}$ must be established. Initially, the square of the molecular field Brillouin function for $S=\frac{5}{2}$ was used for the shape of $f_{\delta V}$. Such a function gave a poor fit for temperatures between 0.3 $T_N$ and $T_N$. However, an alternate procedure can be used to obtain values for the unknown parameters for Eq. (9). Since $\langle \mathbf{S}_i\cdot\mathbf{S}_j\rangle_{\text{nnn}}$ tends towards the saturation, 0°K values of $(2.43)^2$ and $(2.42)^2$ for MnO and MnS, respectively,[7,8] the function $f_{\delta V}$ can properly be set to 1.0 at lower ($<15$°K) temperatures. Hence, using the experimental data above $T_N$ plus those below 15°K (i.e., ignoring data in the region 15°K to $T_N$), a fit to Eq. (9) can be made without assuming any particular shape for $f_{\delta V}$. One proceeds in either of two alternate approaches; (a) in the spirit of the molecular field approximation $\langle \mathbf{S}_i\cdot\mathbf{S}_j\rangle_{\text{nnn}}$ is set to zero in the paramagnetic region or (b) the calculated

[14] Parameters $A$ and $\Theta$ were found to be correlated; procedure adopted for a more rapid convergence treated $\Theta$ as a constant for first two cycles of least squares.

curve based on the random-phase Green's-function approximation by Lines[6] for the paramagnetic region is normalized and employed for $f_{\delta V}$ above $T_N$. Obtaining the thermal-expansion curve in the absence of magnetic interactions, one would be able to determine the nnn correlation curve from the experimental data points below $T_N$ in a region which theoretically would be a difficult problem.

Both of these two alternative procedures, (a) and (b) given above, were applied to the experimental values of the volume-versus-temperature data for MnO and MnS. The values for the parameters used in Eq. (9) are listed in Table I. In Figs. 1 and 3, the solid curves were obtained assuming that $\langle \mathbf{S}_i \cdot \mathbf{S}_j \rangle_{\text{nnn}}$ is zero in the paramagnetic region while the broken curves use values of $f_{\delta V}$ obtained from Lines's values of $\langle \mathbf{S}_i \cdot \mathbf{S}_j \rangle_{\text{nnn}}$ in the paramagnetic region. Note that the broken curve is the correct temperature behavior of the volume for these salts should magnetic interactions be completely absent, and that the difference in volume between the solid and broken curve corresponds to the volume striction arising from short-range order (nnn correlations) in the paramagnetic region. The figures also show dashed curves below $T_N$. Anticipating results given below, these dashed curves were obtained using $f_{\delta V}$ equal to $R_\Delta$, obtained from the trigonal distortion in these salts.

Any approximation which might influence our curve fitting should be examined before conclusions can be made concerning the temperature dependence of the magnetization curves for these two materials. First, the parameter $A$, which is related to $\gamma$, is assumed to be temperature-independent in our fit of Eq. (9) used to remove ordinary thermal expansion of the materials, and it is known that $\gamma$ for some NaCl-structure-type solids changes significantly in the temperature range $0.1\Theta$–$0.2\Theta$. In the case of MnS with $\Theta \cong 275$°K if $\gamma$ should change, this would correspond to data points where the magnetization curve is flat and insensitive (and equal to the saturation value) and, hence, not influence our results. In fact, Fig. 3 shows data points in this temperature range to be nearly identical; hence, any change would be beyond detectability of the present x-ray study. On the other hand, for MnO, the corresponding temperature lies between 45 and 95°K in a temperature region which Fig. 1 cannot provide the same information that Fig. 3 provided for MnS. In addition, this temperature region should contain the more important data points for our magnetization curve. For example, should $\gamma$ change by about 50% in this range, the dashed curve in Fig. 1 would extrapolate to a larger 0°K cell volume and lead to a $\langle \mathbf{S}_i \cdot \mathbf{S}_j \rangle_{\text{nnn}}$ curve with higher relative values in the range 80–120°K.

Comparison with other NaCl-structure solids should allow an estimate of the temperature dependence of $\gamma$. For example, data compiled by Collins and White[15] show similar temperature dependences for the value of $\gamma$ for sodium halides ($\gamma_{2\Theta} \cong 1.6$; $\gamma_{0\text{°K}} \cong 0.93$), a larger temperature dependence for the potassium halides ($\gamma_{2\Theta} \cong 1.47$; $\gamma_{0\text{°K}} \cong 0.30$), and nearly temperature-independent values for LiF and presumably MgO. Furthermore, Collins and White showed that the ratio of elastic stiffness $C_{44}/C_{11}$, and the elastic anisotropy $(C_{11}-C_{12})/2C_{44}$, for different halide members of a particular alkali metal are nearly identical even though within a particular group the individual elastic constants are approximately proportional to the anion radii. With the measured elastic constants for MnO ($C_{11}$, $C_{12}$, and $C_{44}=2.2$, 1.2, and $0.79\times10^{12}$ dyn cm$^{-2}$, respectively,[16] with the similarity of the MgO and MnO lattice constants and $\Theta$, and with the assumption that the elastic constants within a particular group scale as the known interatomic radii, the remaining unknown elastic constants for MnS may be estimated.[17] These, together with a few other pertinent values, are shown in Table II; the values for MnO and MnS suggest a maximum change in the lattice contribution to $\gamma$ of the order of 20%. In the case of MnO the volume (or lattice constant) changes $\sim$1 part in $10^4$ over the temperature range between 45 and 95°K as compared with the strictly volume-exchange-striction change which is about 34 times as large; hence, any error introduced by assumption of constant $\gamma$ is less than 2% of the saturation value. Should this error be of a larger magnitude, it would result in a $\langle \mathbf{S}_i \cdot \mathbf{S}_j \rangle_{\text{nnn}}$ curve which would have a less pronounced falloff in the temperature region 70–120°K. It may be concluded that for our salts, the solid and broken curves[18] in Figs. 1 and 3 closely represent the behavior of the solid either by ignoring the effect of volume striction in the paramagnetic region or

TABLE I. Resulting least-squares parameters used for Figs. 1 and 3.

| | $A$ ($10^{-5}$) | $B$ | $D$ ($10^{-3}$ Å$^3$) | $V_0^{1/3}$(Å) | $\Theta$ (°K) |
|---|---|---|---|---|---|
| MnO[a] | 3.42 | 30.6 | 3.41 | 4.4350 | 424.8 |
| MnS[a] | 5.95 | 1.0 | 4.92 | 5.2019 | 272.6 |
| MnO[b] | 3.07 | 39.0 | 4.92 | 4.4367 | 425.4 |
| MnS[b] | 5.58 | 0.9 | 6.01 | 5.2044 | 273.0 |

[a] These values are obtained if no next-nearest-neighbor spin correlation is assumed in the paramagnetic temperature region.
[b] These values are obtained using $\langle \mathbf{S}_i \cdot \mathbf{S}_j \rangle_{\text{nnn}}$ from Ref. 7 in the paramagnetic region.

[15] J. G. Collins and G. K. White, Progr. Low Temp. Phys. 4, 450 (1964).

[16] D. W. Oliver, J. Appl. Phys. **40**, 893 (1969).

[17] Since the more conventional ultrasonic technique for determination of elastic constants requires large single crystals, values for MnS, which is usually available only as a powder, probably will be measured only by a technique such as thermal diffuse x-ray scattering [W. A. Wooster, *Diffuse X-ray Reflections from Crystals* (Oxford University Press, London, 1962)]. The values for MnO may be compared with those determined for CoO by K. S. Aleksandrov, L. A. Shabanova, and L. M. Reshchikova, Fiz. Tverd. Tela **6**, 1666 (1968) [English transl.: Soviet Phys.—Solid State **10**, 1316 (1968)] which are (in units $10^{12}$ dynes cm$^{-2}$) $C_{11}=2.62$, $C_{12}=1.45$, and $C_{44}=0.832$. Thus $C_{44}/C_{11}$ is 0.316 and $(C_{11}-C_{12})/2C_{44}$ is 0.705.

[18] Thermal-expansion coefficients, $\alpha=\Delta l 10^6/l\Delta T$, are 14.2, 9.6, and 2.42 for MnO, and 20.5, 18.3, and 12.5 for MnS at 285, 150, and 80°K, respectively.

TABLE II. Elastic-constant data for fcc salts.

| | $C_{11}$[a] | $C_{12}$[a] | $C_{44}$[a] | $C_{44}/C_{11}$ | $(C_{11}-C_{12})/2C_{44}$ | $\gamma$[b] | $\gamma_0$°K |
|---|---|---|---|---|---|---|---|
| MnO | 2.20[c] | 1.20[c] | 0.79[c] | 0.36[d] | 0.63 | | |
| MnS | 1.43 | 0.74 | 0.52 | 0.36[d] | 0.66[e] | 1.6[f] | |
| LiF[g] | 1.13 | 0.476 | 0.637 | 0.56 | 0.52 | 1.60 | 1.65 |
| MgO[g] | 2.89 | 0.857 | 1.55 | 0.54 | 0.65 | 1.52 | ... |
| KCl[g] | 0.403 | 0.066 | 0.063 | 0.15 | 2.68 | 1.45 | 0.32 |
| KBr[g] | 0.346 | 0.058 | 0.051 | 0.14 | 2.85 | 1.47 | 0.30 |
| KI[g] | 0.271 | 0.045 | 0.036 | 0.24 | 3.10 | 1.49 | 0.28 |
| NaCl[g] | 0.483 | 0.127 | 0.128 | 0.26 | 1.39 | 1.57 | 0.93 |
| NaI[g] | 0.301 | 0.091 | 0.073 | 0.24 | 1.44 | 1.72 | 0.93 |

[a] Units are $10^{-12}$ dynes cm$^{-2}$.
[b] Values at 285°K given here; those for LiF and MgO may be slightly in error.
[c] Ref. 16.
[d] Value for MnO from observed values; that for MnS assigned.
[e] Value is about 4% larger than that for MnO because of increase in the anion radius.
[f] I. Wakabayashi, H. Kobayashi, H. Nagasaki and S. Minomura, J. Phys. Soc. Japan **25**, 227 (1968).
[g] Values in table for these salts from Ref. 15.

including such a contribution equal to that calculated on the basis of the $\langle \mathbf{S}_i \cdot \mathbf{S}_j \rangle_{\text{nnn}}$ curve determined by Lines and Jones, respectively. By subtracting the experimental data points from the calculated curve (broken line in Fig. 1), experimental values for $\langle \mathbf{S}_i \cdot \mathbf{S}_j \rangle_{\text{nnn}}$ can be determined. These results are shown in Fig. 7. As previously indicated, no theoretical results are available for comparison with these data.

It is interesting to note that if the solid curve in Fig. 1 for MnO is used, the data below $T_N$ yields a magnetization curve which is almost identical to that found from the trigonal distortion. These data are shown in Fig. 8 as solid points; also shown are the corresponding data including spin correlation in the paramagnetic region. The same solid curves calculated by Lines and Jones and used in Fig. 5 are shown. Values of $R_{\delta a}$, where $R_{\delta a}=[(\delta a/a)_T/(\delta a/a)_{0°\text{K}}]^{1/2}$, follow the $j/J_2=0.01$ curve as was the case for $R_\Delta$. Hence, use of $R_\Delta$ for $f_{\delta V}$ to obtain the dashed curve in Fig. 1 appears justified.

The corresponding results for MnS are shown in Fig. 9. Again the data are situated about the $P=0.02$ curve as was the case for the data in Fig. 6. However, in this case the fit in the region 0.8 to 1.0 $T_N$ is not as good as that for $R_\Delta$ data. As was previously pointed out, a distortion parameter an order of magnitude smaller than that in MnO would satisfy these experimental results. It appears that even for MnS, the salt believed to be most suitable in which to study biquadratic-exchange effects, the experimental results do not require such effects to be invoked.

Table III summarizes the values of $\delta a/a$ and $\Delta$ obtained for MnO and MnS at 0°K. The values for $\delta a/a$ included in this table are those obtained with inclusion of volume exchange-striction term in the paramagnetic region. Together with the exchange constants previously determined for these materials and the estimated elastic constants from Table II, values for $\epsilon$, the logarithmic derivatives of the exchange constants have been determined and are included in Table III.

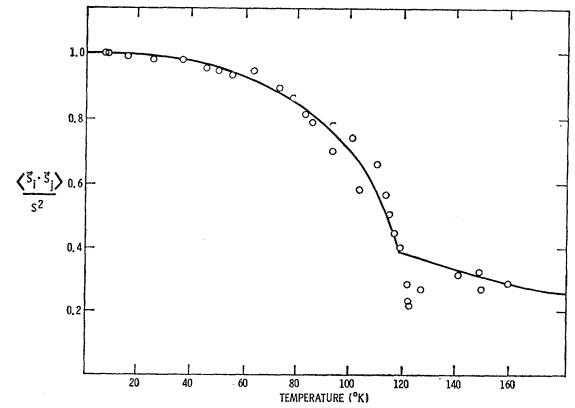


FIG. 7. Experimental $\langle \mathbf{S}_i \cdot \mathbf{S}_j \rangle_{\text{nnn}}$ curve obtained from the observed volume striction observed in MnO. Above $T_N$ the values calculated by Lines (Ref. 6) have been normalized to the saturation value of $S$ (=2.43).

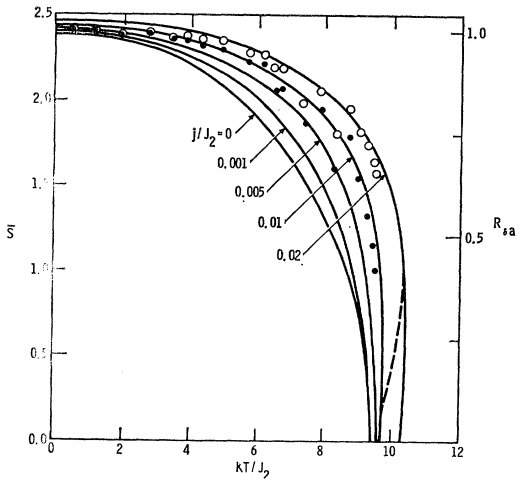


FIG. 8. The value of $R_{\delta a}$ for MnO determined in this study. The values, $R_{\delta a}=[(\delta a/a)_T/(\delta a/a)_{0°\text{K}}]^{1/2}$ are plotted against the same curves used in Fig. 5. Solid points are obtained ignoring volume contraction in the paramagnetic region; open circles are for values obtained using the Lines $\langle \mathbf{S}_i \cdot \mathbf{S}_j \rangle_{\text{nnn}}$ curve in the paramagnetic region in addition to normal thermal expansion. These data closely fit the $j/J_2=0.01$ distortion parameter curve in the same manner as the $R_\Delta$ data in Fig. 5.

TABLE III. Exchange-striction and related parameters.

| | MnO | MnS |
|---|---|---|
| $\delta a/a$ (at 0°K) | $1.1\times10^{-3}$ | $1.2\times10^{-3}$ |
| $\Delta$ (at 0°K) | $1.1\times10^{-2}$ | $1.72\times10^{-3}$ |
| $J_1$ (°K) | −10 | −7 |
| $J_2$ (°K) | −11 | −12.5 |
| $\epsilon_1$ | −23 | −5.5 |
| $\epsilon_2$ | 12.4 | 12.2 |

In summary, the most important conclusions of this paper are the experimental observation of a contraction along the threefold axis for MnS below $T_N$ and the determination of the trigonal distortion $\Delta$ in MnO to confirm the magnetization curve calculated by Lines and Jones. In addition, a nnn spin-correlation function is experimentally obtained which might stimulate theoretical interest in this problem. Finally, results on MnS suggest, though not conclusively prove, that a "biquadratic-exchange" effect is probably too small to be detected by the x-ray method.

*Note added in proof.* We missed the recent lattice constant data on MnO [D. Block, P. Charbit, and R. Georges, Compt. Rend. **266B**, 430 (1968)] and on MnS [R. Georges, Compt. Rend. **268B**, 16 (1969)]. Georges did not observe the trigonal distortion for MnS. Our values, measured with a slightly greater precision, are in good agreement with these more limited data. Calculations have been carried out on near neighbor correlation functions for MnO [L. C. Bartel, Phys. Rev. **B1**, 1254 (1970)].

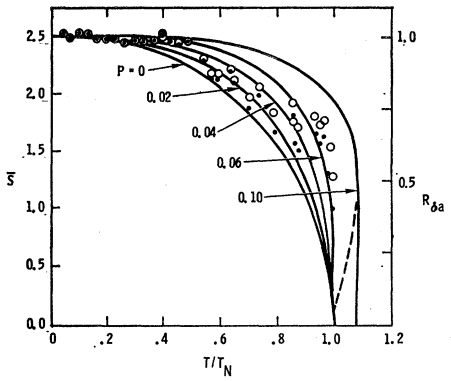


FIG. 9. The value of $R_{\delta a}$ for MnS versus $T/T_N$. The experimental values, $R_{\delta a}=[(\delta a/a)_T/(\delta a/a)_{0°K}]^{1/2}$, are shown on the same calculated curves which appear in Fig. 6. Solid points are obtained ignoring volume contraction in the paramagnetic region; open circles are for values using Jones $\langle \mathbf{S}_i\cdot\mathbf{S}_j\rangle_{nnn}$ in the paramagnetic region. Below 0.8 $T/T_N$ the solid points fit the $P=0.02$ biquadratic parameter curve in the same manner as the $R_\Delta$ data in Fig. 6; open circles fit a slightly larger $P$ value (0.04). These data as well as those for $R_\Delta$ of Fig. 6 will give an excellent fit on a $j/J_2=0.001$ distortion parameter curve calculated by Lines and Jones (Ref. 7) suggesting that the biquadratic-exchange effect may not be required even for MnS.

## ACKNOWLEDGMENTS

The author wishes to acknowledge R. A. Trudo for technical assistance. He is particularly indebted to E. D. Jones for suggesting this problem and for his stimulating and helpful discussions. He also wishes to thank Dr. M. E. Lines and Dr. L. C. Bartel for comments regarding the text of the manuscript.